Available online at www.sciencedirect.com
ScienceDirect
European Journal of Mechanics B/Fluids 27 (2008) 54–61

Elementary properties of the enstrophy and strain fields in confined two-dimensional flows

L. Zavala Sansón *, J. Sheinbaum

Department of Physical Oceanography, CICESE, Ensenada, Baja California, Mexico

Received 4 September 2006; received in revised form 23 March 2007; accepted 5 April 2007

Available online 4 May 2007

Abstract

The evolution of decaying two-dimensional turbulent flows in a bounded domain is considered. It is shown that the global enstrophy is always equal to the total squared strain field, when integrated over a domain with no-slip boundaries, despite the complex evolution of the flow and strong vortex-wall interactions. This property is also valid for a square domain with stress-free walls, and in general for any polygonal boundary. In contrast, the enstrophy is always greater than the squared strain field in a stress-free circular domain, and in general for any closed domain with negatively-signed curvature at all points of the boundary.

Keywords: 2D turbulence; Enstrophy; Boundary conditions

1. Introduction

The evolution of a two-dimensional (2D) turbulent flow is characterized by an inverse energy cascade, transferring energy from small scales of motion towards larger scales, and a direct enstrophy cascade [1,2]. This process is better understood for inviscid flows, in which global energy and enstrophy are conserved quantities. In order to consider such flows, early studies on 2D turbulence focused on theoretical models and numerical simulations with periodic boundary conditions and high Reynolds numbers [3–5]. Other applications consider the motion of homogeneous fluid in a constantly rotating system, where the flow presents columnar (and therefore 2D) behavior, as derived from the Taylor–Proudman theorem [6].

The role of lateral walls on the evolution of confined, turbulent flows has been the subject of recent experimental and numerical investigations [7–10]. These studies have shown the role of solid boundaries on the self-organization of small eddies into larger vortices that characterizes the freely decaying turbulence (with dissipation and no forcing). Again, the enstrophy cascade is a key element in these processes. Considering the Cartesian plane of motion (x, y) the relative vorticity field for a 2D flow is defined as $\omega = v_x - u_y$, where $\mathbf{u} = (u, v)$ is the velocity vector and subindices denote partial derivatives. The time evolution of the total enstrophy, $Z = 1/2 \int \omega^2 \, \mathrm{d}A$, in a finite domain with area A and no-slip boundaries is

* Corresponding author.
E-mail address: izavala@cicese.mx (L. Zavala Sansón).

0997-7546/$ – see front matter
doi:10.1016/j.euromechflu.2007.04.002

$$\frac{\mathrm{d}Z}{\mathrm{d}t} = -\nu \int |\nabla\omega|^2 \,\mathrm{d}A + \nu \oint \omega(\nabla\omega \cdot \hat{\mathbf{n}}) \,\mathrm{d}l. \tag{1}$$

The first integral on the right hand-side is the palinstrophy, whilst the second integral (along the contour of the domain) is associated with the production of vorticity at the wall. This term represents an important contribution due to the boundaries, and it is obviously not considered in studies for unbounded flows. Even though there might be local production of vorticity, it must be recalled that the total circulation of the flow vanishes $\int \omega \,\mathrm{d}A = 0$. This is not the case for stress-free walls, where there is net vorticity flux through the walls [8]. Note also that if the flow is unbounded, the enstrophy is a monotonically decaying functional since the palinstrophy is always positive. In the presence of boundaries, however, the enstrophy is also decaying but not monotonically, due to vorticity production at the walls (see e.g. [11]).

The emergence of vortical structures during the flow evolution has led to efforts to characterize regions dominated by the presence of vortices. One of these criteria is the Okubo–Weiss function [12,13]

$$Q = s_1^2 + s_2^2 - \omega^2, \tag{2}$$

where the strain components are defined as $s_1 = u_x - v_y$ and $s_2 = u_y + v_x$. Basically, $Q(x, y, t)$ compares the rotation ($Q < 0$) and the strain ($Q > 0$) dominated regions. Evidently, strong negative values of Q are found at the core of vortices, while outside regions are characterized by small (positive and negative) Q values; strong positive values can also be found surrounding the vortices [14,15]. Although there has been some criticism [16] the Okubo–Weiss function provides a simple way to characterize the different regions of the flow, and to identify vortical structures [17].

In this short paper a number of global properties of Q are shown, which have not been noticed or sufficiently discussed in previous studies. An important property is that Q is identically zero when integrated over a domain with no-slip walls, which implies that the total enstrophy is equal to the total squared strain $S = 1/2 \int (s_1^2 + s_2^2) \,\mathrm{d}A$ at all times. This is shown in particular for a simulation of decaying 2D turbulence in a square domain (Section 1). Afterwards, the global value of Q is analyzed for simple domains with stress-free walls (Section 2). It shall be shown that this quantity is also zero for a square domain with stress-free boundaries. In contrast, that result is not valid for a stress-free circular domain, where the total enstrophy is always greater than the total squared strain. Furthermore, the global value of Q is examined for any closed domain with arbitrary shape and boundary conditions (Section 4). Section 5 is a summary and discussion of the main results of the paper.

2. Domains with no-slip boundaries

In order to derive global properties of the Okubo–Weiss function, it is important to notice that Q can be written in terms of the determinant of the velocity gradient by decomposing this tensor into its symmetric and antisymmetric parts

$$\nabla\mathbf{u} = \frac{1}{2}\begin{pmatrix} s_1 & s_2 \\ s_2 & -s_1 \end{pmatrix} + \frac{1}{2}\begin{pmatrix} 0 & -\omega \\ \omega & 0 \end{pmatrix}, \tag{3}$$

which implies that

$$\det(\nabla\mathbf{u}) = -\frac{1}{4}\left(s_1^2 + s_2^2 - \omega^2\right) \equiv -\frac{1}{4}Q. \tag{4}$$

The function Q vanishes when integrated over the whole domain with no-slip walls. This elementary property can be derived by noticing that the divergence of the acceleration vector $D\mathbf{u}/Dt$, with D/Dt the material derivative, is proportional to the determinant of the velocity gradient, and is therefore also related with Q:

$$\nabla \cdot (\mathbf{u} \cdot \nabla\mathbf{u}) = -2\det(\nabla\mathbf{u}) \equiv \frac{1}{2}Q. \tag{5}$$

(By definition $\nabla \cdot \bar{u} = 0$.) Integrating over the whole domain and applying the Gauss theorem yields

$$\oint (\mathbf{u} \cdot \nabla\mathbf{u}) \cdot \hat{\mathbf{n}} \,\mathrm{d}l = \frac{1}{2}\int Q \,\mathrm{d}A. \tag{6}$$

Therefore, $\int Q \,\mathrm{d}A = 0$ for no-slip boundaries, where the velocity components are zero, regardless of the shape of the domain.

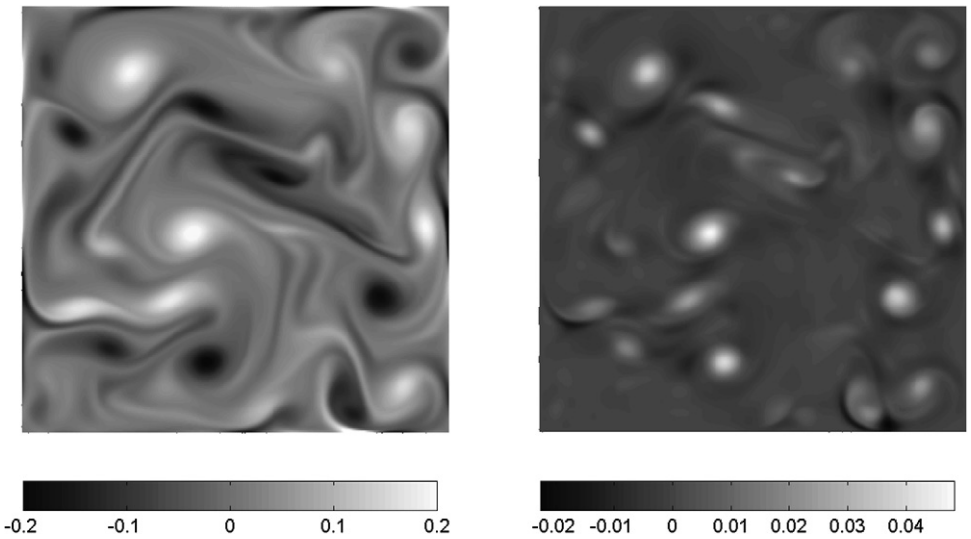

Fig. 1. Left: Vorticity surfaces calculated at $t = 400$ from a simulation in a squared domain with no-slip boundaries ($Re = 2500$). Right: Corresponding surfaces of the (minus) Okubo–Weiss function $-Q = \omega^2 - (s_1^2 + s_2^2)$.

Note that this result is also obtained by writing the determinant of the velocity gradient as the divergence of a vector whose components depend on the velocity field (this procedure will be useful when analyzing stress-free boundary conditions):

$$\det(\nabla \mathbf{u}) = \frac{1}{2}\nabla \cdot (uv_y - vu_y, vu_x - uv_x). \tag{7}$$

Integrating Q and then applying the Gauss theorem and the no-slip condition it is verified that

$$\int Q \,\mathrm{d}A = -2 \oint (uv_y - vu_y, vu_x - uv_x) \cdot \hat{\mathbf{n}} \,\mathrm{d}l = 0. \tag{8}$$

As a result, the total enstrophy (Z) is equal to the total squared strain (S) at all times

$$\frac{1}{2}\int \omega^2 \,\mathrm{d}A = \frac{1}{2}\int \left(s_1^2 + s_2^2\right) \mathrm{d}A. \tag{9}$$

Thus, despite squared vorticity and strain fields are locally very different in most parts of the domain, they have always the same value globally. Furthermore, the time evolution of the total squared strain is also given by Eq. (1). It is important to emphasize that $\int Q \,\mathrm{d}A = 0$ in a bounded, no-slip domain is a kinematical property, since it is derived from the velocity gradient and not from the momentum equations.

In order to show characteristics of the two contributors to $\int Q \,\mathrm{d}A$, the vorticity equation is numerically integrated using a finite differences code [18]. The scheme is based on a vorticity-stream function formulation, where $\omega = -\nabla^2\psi$, and the stream function ψ is defined from the continuity equation such that $u = \psi_y$ and $v = -\psi_x$. Using non-dimensional units, the domain is a squared box with sidelength $L = 1$ and with a horizontal resolution of 256×256 grid points. The initial condition is an array of 16×16 Gaussian vortices with radius $r = 0.025$ and alternate signed vorticity with magnitude $|\omega_{\max}| = 1$. Within a space of length $2r$ between the closest row (column) of vortices and the boundaries there is no vorticity. The arrangement of the vortices is not uniform: their positions have a small random perturbation of about $0.5r$ (a similar procedure was followed in other studies [8]). Several simulations with different perturbations were performed in order to verify the results for different initial conditions. The Reynolds number is $Re = 2500$, based on the initial $U_{\mathrm{rms}} = 0.005$ of the velocity field and on the half-length of the domain $L/2 = 0.5$ (using $\nu = 10^{-6}$).

Fig. 1(a) shows the vorticity surfaces at time $t = 400$ in a typical simulation, when the flow has already organized into relatively large vortices, according to the inverse energy cascade. At this stage, the basic interactions commonly observed in 2D turbulence are clearly captured: vortices with equal sign merge, while vortices with different sign form dipolar structures and propagate through the domain. Furthermore, due to the no-slip boundary condition strong

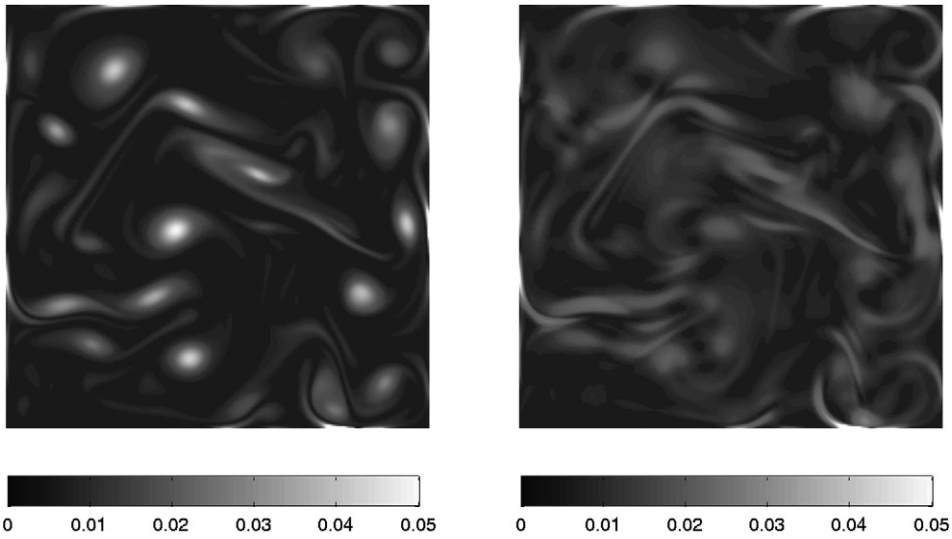

Fig. 2. Numerically calculated surfaces of the enstrophy (left) and squared strain fields (right) at $t = 400$. Maximum values at the boundary are approximately 0.4.

vorticity filaments ejected from the walls are clearly visible. They arise from intense interactions of the flow with the walls: in the presence of cyclonic or anticyclonic vortices, a strong filament of opposite vorticity is produced at the boundary. Fig. 1(b) presents the corresponding surfaces of the (minus) Okubo–Weiss function $-Q$. Large positive $-Q$ values indicate the presence of rotation-dominated regions associated with vortical structures, while strong negative values indicate those regions where the strain predominates over the vorticity. It can be noticed that the vorticity filaments ejected from the wall (visible in Fig. 1(a)) are dominated by strain. This means that despite strong vorticity production during vortex-wall interactions, strain eventually dominates these regions. This behaviour indicates that the role of no-slip walls as a source of vortices [10] into the interior of the flow domain might be more limited than expected.

Figs. 2(a) and 2(b) represent surfaces of ω^2 and $s_1^2 + s_2^2$, respectively, which have the same global value, according to (9). Notice that the ω^2 field is rather different than the $s_1^2 + s_2^2$ surfaces, except near the walls, where they cancel each other (i.e. Q is zero at ∂A). For instance, at the eastern wall $u_y = v_y = u_x = 0$ and $v_x \neq 0$, which implies that $s_1 = 0$ and $\omega^2 = v_x^2 = s_2^2$. This does not mean, however, that enstrophy or squared strain have a low value next to the walls. On the contrary, it is in these regions where the production of vorticity and deformation due to strain is more intense [10]. This strong enstrophy production at the walls is due to the advection of vortices towards the wall, and has been thoroughly studied in numerical simulations [8,9]. As noted before, when these filaments are ejected from the boundary into the domain, they turn into strain-dominated regions. Observe also that the vorticity and strain values at the wall are much larger than values inside the domain.

In order to have a more complete idea of the field distributions, Fig. 3 shows the normalized histograms of local enstrophy and squared strain using bins of 0.002 for three different times. From this distribution the flow can be characterized by four distinctive regions. Region 1 includes grid points of the domain having very small values of enstrophy and squared strain, the amount of low-enstrophy points being slightly larger. Region 2 corresponds with the periphery of visible vortices in previous figures, where there are more areas with squared strain greater than enstrophy. Less numerous grid points in region 3 are clearly dominated by vortices, where enstrophy is greater than squared strain. Finally, very few regions next to the walls possess the highest values. These field distributions were found to be very similar for simulations with Reynolds number 1000 and 5000 (not shown here).

3. Square and circular domains with stress-free boundaries

Now the global Q is analyzed for stress-free boundary conditions, that is, when the walls do not exert friction on the fluid. Essentially, this condition states that $(\boldsymbol{\tau} \cdot \hat{\mathbf{n}})_{||} = 0$, where $\boldsymbol{\tau}$ is the stress tensor and the vertical lines indicate the component parallel to the boundary [19]. A remarkable difference with a no-slip domain is that there might be a

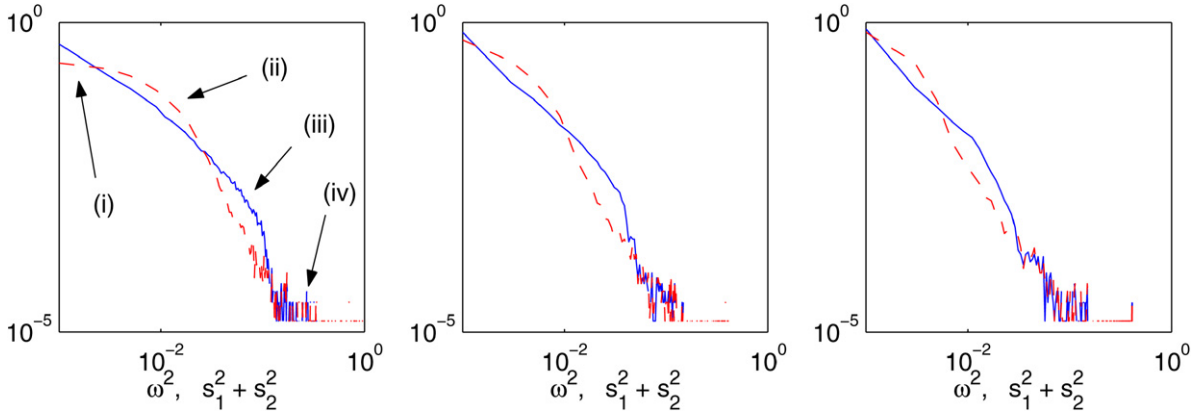

Fig. 3. Normalized histograms of enstrophy (continuous) and squared strain fields (dashed) into 0.002 wide classes for three different times $t = 200, 400, 600$ (second panel corresponds with simulation presented in Figs. 1 and 2). Arrows indicate regions associated with (ii) the periphery of vortices, (iii) vortices, and (iv) high values at the walls.

net leakage of vorticity through the stress-free boundaries [8]. Consider first the square domain, where $v = v_x = 0$ at the horizontal boundaries, and $u = u_y = 0$ at the left and right walls. By writing the global Q as in (8), it is found that the line integrals corresponding to the four boundaries vanish, implying that $\int Q\,\mathrm{d}A = 0$ again. Note that this result is just a consequence of the impermeability of the walls. The stress-free condition states that $v_x = 0$ ($u_y = 0$) at the vertical (horizontal) walls. As a result, $\omega = 0$ at the boundaries [19].

It is important to point out, however, that $\int Q\,\mathrm{d}A = 0$ does not necessarily hold for a stress-free boundary with a different geometry. This is the case of a circular domain with radius R. Using polar coordinates (r, θ) and denoting radial and azimuthal velocities as (u, v), the determinant of the velocity gradient can be written as the divergence of a vector whose components depend on the velocity field, analogous to expression (7):

$$\det(\nabla \mathbf{u}) = \frac{1}{2}\nabla \cdot \left(\frac{1}{r}\left(uv_\theta - vu_\theta + u^2 + v^2\right), vu_r - uv_r\right), \tag{10}$$

where the nabla operator is in polar coordinates. Using (4), integrating over the whole domain and applying the Gauss theorem, the global Q can be calculated again as a contour integral

$$\int Q\,\mathrm{d}A = -2\oint \left(\frac{1}{R}\left(uv_\theta - vu_\theta + u^2 + v^2\right), vu_r - uv_r\right) \cdot \hat{\mathbf{i}}_\mathbf{r} R\,\mathrm{d}\theta, \tag{11}$$

where $\hat{\mathbf{i}}_\mathbf{r}$ is the radial unit vector pointing outward the circular boundary. Of course, this integral is zero for no-slip conditions ($u = v = 0$ at the boundary), as expected. By noticing that $u = u_\theta = 0$ and in general $v \neq 0$ at a stress-free wall, this expression reduces to

$$\int Q\,\mathrm{d}A = -2\oint v^2\,\mathrm{d}\theta < 0. \tag{12}$$

Recalling the definition $\int Q\,\mathrm{d}A = 2(S - Z)$, it is then concluded that the total enstrophy is greater than the total strain field, $Z > S$. Analogously to the square domain, the stress-free boundary imposes a condition for the vorticity, $\omega = 2v/R$ at the wall [19], and then $\int Q\,\mathrm{d}A = -R^2/2\oint \omega^2\,\mathrm{d}\theta$. As a simple example, consider a flow with uniform relative vorticity over the whole circular domain $\omega = -2\Omega$ for all (r, θ), with Ω constant. By straightforward calculations it can be verified that $s_1 = s_2 = 0$ and therefore

$$\int Qr\,\mathrm{d}r\,\mathrm{d}\theta = -4\pi\Omega^2 R^2 < 0. \tag{13}$$

4. Arbitrary domains with stress-free conditions

It is possible to analyze previous results from a more general perspective for arbitrary domains with stress-free boundaries. Consider the boundary domain as a smooth (differentiable in every point), closed curve that does not intersect itself. The flow domain A and its boundary ∂A can be defined as [20]:

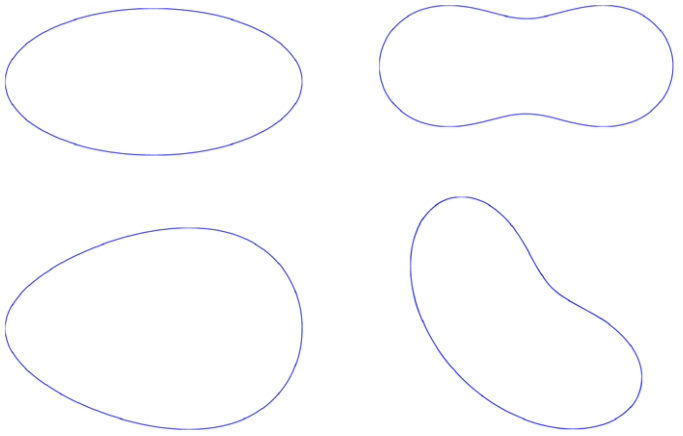

(a) (b)

Fig. 4. (a) Closed domains with negative curvature at all points of the boundary (ellipse and *egg* curve). (b) Domain boundaries with positive and negative curvature at different points (Cassini oval and *bean* curve).

$$A = \{\mathbf{x} \in \mathrm{R}^2;\ f(\mathbf{x}) > 0\},$$
$$\partial A = \{\mathbf{x} \in \mathrm{R}^2;\ f(\mathbf{x}) = 0\}, \tag{14}$$

where $f(\mathbf{x})$ is a function in $\mathbb{R}^2$ marking the boundary of the domain, and defining the normal vector $\hat{\mathbf{n}} = -\nabla f/|\nabla f|$. Substituting $\hat{\mathbf{n}}$ in (6), integrating by parts and using index notation, the global Q is

$$\int Q\,\mathrm{d}A = 2\oint \frac{1}{|\nabla f|}\frac{\partial^2 f}{\partial x_i \partial x_j} u_i u_j\,\mathrm{d}l \tag{15}$$

where $(i = 1, 2;\ j = 1, 2)$. An equivalent expression was pointed out in [13], where some comments on the influence of the boundary shape for the sign of $\int Q\,\mathrm{d}A$ were made. Here we explicitly show some further considerations related not only to the shape of the boundary, but also to the boundary conditions. Note that for general surfaces the integrand $(\partial^2 f/\partial x_i \partial x_j)u_i u_j$ is the second fundamental form of ∂A and is therefore directly related with the local curvature of the domain. For a closed geometry different situations may occur, depending on the value of the discriminant $B = \det(\partial^2 f/\partial x_i \partial x_j)$ [21].

First, consider the situation where $B > 0$, which implies that values of the curvature at all points of the boundary have the same sign. In this case, the line integral (15) is either positive or negative definite. For a closed geometry as the type considered here (with the normal vector pointing outwards and the line integral evaluated counter-clockwise) this integral can only be negative definite, which corresponds with a closed domain with negative curvature at all boundary points. This is the case of a circular or oval domain, for example, as shown in Fig. 4(a). (Note that the opposite situation, a smooth boundary with positive curvature at all points, cannot occur in a closed domain.)

Consider for instance an elliptical domain with its boundary defined as

$$f(x, y) = -\frac{x^2}{a^2} - \frac{y^2}{b^2} + 1 \equiv 0, \tag{16}$$

so the normal vector is

$$\hat{\mathbf{n}} = \frac{1}{2\sqrt{x^2/a^4 + y^2/b^4}}\left(\frac{2x}{a^2}, \frac{2y}{b^2}\right). \tag{17}$$

The discriminant B is calculated with the second derivatives

$$\frac{\partial^2 f}{\partial x^2} = -\frac{2}{a^2}, \qquad \frac{\partial^2 f}{\partial y^2} = -\frac{2}{b^2}, \qquad \frac{\partial^2 f}{\partial x \partial y} = 0 \tag{18}$$

which yields $B = 4/(a^2 b^2) > 0$. Thus, the global Q is find to be negative

$$\int Q\,\mathrm{d}A = -2\oint \frac{1}{\sqrt{x^2/a^4 + y^2/b^4}}\left(\frac{u^2}{a^2} + \frac{v^2}{b^2}\right)\mathrm{d}l < 0 \tag{19}$$

or, equivalently, $Z > S$. Note that for $a = b = R$ (that is, a circular domain) and changing to polar coordinates the result (12) is recovered.

On the other hand, if $B < 0$ then the line integral is not positive or negative definite, and therefore the sign of the global Q is unknown. This is the case for domains with boundaries whose curvature changes sign, so it is positive at some points and negative at some others. Fig. 4(b) shows examples of well-known curves with such characteristics.

It must be noted that these arguments cannot be directly applied for polygonal domains, i.e. with straight walls, since this type of boundary is not differentiable at sharp corners (i.e. it is not smooth). However, it is important to point out that for any closed, polygonal domain boundaries it is verified that global Q is also zero and that the stress-free condition implies that ω is zero at the straight walls, as shown for the case of a square domain. This can be derived by writing equation (6) as a sum of line integrals along the polygonal boundary with $N > 2$ walls

$$\int Q \,\mathrm{d}A = 2 \sum_{k=1}^{N} \oint (uu_x + vu_y, uv_x + vv_y) \cdot \hat{\mathbf{n}}_k \,\mathrm{d}l, \tag{20}$$

where $\hat{\mathbf{n}}_k$ is the corresponding unit vector for each wall. A suitable rotation of coordinates by an angle α_k can be applied when calculating each line integral such that the boundary conditions in the rotated frame are expressed as $v' = v'_{x'} = u'_{y'} = 0$, and $\hat{\mathbf{n}}_k = (\sin\alpha_k, -\cos\alpha_k)$. [Note that the case $\alpha = 0$ corresponds with a horizontal wall, where $v = v_x = u_y = 0$ and $\hat{\mathbf{n}} = (0, -1)$.] After some cumbersome but direct calculations it follows that all individual contributors of the sum of line integrals are zero, and therefore $\int Q \,\mathrm{d}A = 0$. By following the same procedure, it is also found that the vorticity is zero at every point of the straight walls, as expected from the square domain case.

5. Final remarks

Summarizing, it has been shown that for a flow confined within no-slip boundaries with arbitrary geometry $\int Q \,\mathrm{d}A$ is identically zero. An important consequence is that the squared vorticity (enstrophy) and strain fields have globally the same value, $Z = S$. This is somewhat surprising considering that ω^2 and $s_1^2 + s_2^2$ are locally very different fields at any time, as shown in Fig. 2 for a no-slip square domain. It was also found that these fields are identical at the no-slip walls, and that the strong filaments ejected from the boundaries are slightly strain-dominated regions. Although such filaments contain high vorticity values compared with vortices in interior regions of the domain, strain values are even larger. Thus, as a direct consequence of the global property $Z = S$ over the whole domain, the intense generation of enstrophy at the walls is balanced by the associated strain production. Therefore, it might be expected that high-vorticity filaments erupted from the walls do not necessarily transform into new vortices in the interior, i.e. there cannot be an unbounded growth of vorticity-dominated structures generated at the walls.

In contrast with no-slip walls the vanishing of the global Okubo–Weiss function is not valid for a flow confined within a stress-free circular boundary. In this case, $\int Q \,\mathrm{d}A < 0$, implying that $Z > S$ at all times. Furthermore, this situation also applies for any smooth, closed domain with negative curvature at every point of the boundary (see Fig. 4). When the line integral is not positive or negative definite (which implies positive or negative curvature values along the boundary) it is not possible to determine whether this condition prevails. On the other hand, if the stress-free domain has straight walls (such as a square container) then it is verified that the global Q is zero and the vorticity is null at the boundary.

A question that naturally arises is to what extent these properties help to explain the differences on the self-organization process observed for different boundary conditions and domain geometries [7–9]. The global character of the Q field properties makes difficult to determine such differences, except perhaps for no-slip boundaries, where high-enstrophy and squared strain values are concentrated (due to viscous stresses) and balanced (in order to keep $Z = S$) at the walls. In contrast, these fields are not necessarily balanced at a stress-free boundary, as can be observed from the simulations in [8] for a square container. Thus, values of the Q field at this type of boundary could provide additional information on the qualitative character of the flow in the rest of the domain (e.g. the distribution of enstrophy and squared strain). On the other hand, it is remarkable that the global Q is not zero for some particular geometries (such as circular or elliptical domains, where $Z > S$), whereas it is not possible to determine the sign of $\int Q \,\mathrm{d}A$ for flow domains with both convex and concave boundary sections. The influence of the domain geometry on the self-organization of the flow should be examined, which will require to further analyze the results of simulations with stress-free circular boundaries (which are rather scarce, e.g. [7]), and to perform new simulations with more complicated geometries, which is beyond the scope of this paper.

There are two additional considerations that are worth mentioning. First, the property $\int Q\,\mathrm{d}A = 0$ is also valid for periodic boundaries. Note that the global Q can be expressed in terms of the stream function as $\int Q\,\mathrm{d}A = 4\int(\psi_{xy}^2 - \psi_{xx}\psi_{yy})\,\mathrm{d}A$, and let ψ be proportional to periodic modes $\psi_0 \exp[\mathrm{i}(kx + ly)]$. Then $\int Q\,\mathrm{d}A \propto 4\sum_{k,l}[(kl)^2 - k^2l^2]\psi_0^2 = 0$. Second, the derived global properties of Q are kinematical, which implies that they are valid regardless of the imposed dissipation or forcing in the vorticity equation. This is the case when the flow is affected by different dissipative dynamics, instead or in addition to Laplacian diffusion, e.g. by bottom friction effects [18].

References

[1] R.H. Kraichnan, Inertial ranges in two-dimensional turbulence, Phys. Fluids 10 (1967) 1417–1423.
[2] G.K. Batchelor, Computation of the energy spectrum in homogeneous two-dimensional turbulence, Phys. Fluids Suppl. II 12 (1969) 233–239.
[3] U. Frisch, P.L. Sulem, Numerical simulation of the inverse energy cascade in two-dimensional turbulence, Phys. Fluids 27 (1984) 1921–1923.
[4] J.C. McWilliams, The emergence of isolated coherent vortices in turbulent flow, J. Fluid Mech. 146 (1984) 21–43.
[5] P. Santangelo, R. Benzi, B. Legras, The generation of vortices in high-resolution, two-dimensional decaying turbulence and the influence of initial conditions on the breaking of self-similarity, Phys. Fluids A 1 (1989) 1027–1034.
[6] E.J. Hopfinger, G.J.F. van Heijst, Vortices in rotating fluids, Annu. Rev. Fluid Mech. 25 (1993) 241–289.
[7] S. Li, D. Montgomery, W.B. Jones, Two-dimensional turbulence with rigid circular walls, Theor. Comput. Fluid Dyn. 9 (1997) 167–181.
[8] H.J.H. Clercx, S.R. Maassen, G.J.F. van Heijst, Decaying two-dimensional turbulence in square containers with no-slip or stress-free boundaries, Phys. Fluids 11 (1999) 611–626.
[9] S.R. Maassen, H.J.H. Clercx, G.J.F. van Heijst, Self-organization of quasi-two-dimensional turbulence in stratified fluids in square and circular containers, Phys. Fluids 14 (2002) 2150–2169.
[10] H.J.H. Clercx, G.J.F. van Heijst, D. Molenaar, M.G. Wells, No-slip walls as vorticity sources in two-dimensional bounded turbulence, Dyn. Atmos. Oceans 40 (2005) 3–21.
[11] H.J.H. Clercx, C.H. Bruneau, The normal and oblique collision of a dipole with a no-slip boundary, Comp. Fluids 35 (2006) 245–279.
[12] A. Okubo, Horizontal dispersion of floatable particles in the vicinity of velocity singularities such as convergences, Deep-Sea Res. 17 (1970) 445–454.
[13] J. Weiss, The dynamics of enstrophy transfer in two-dimensional hydrodynamics, Physica D 48 (1991) 273–294.
[14] D. Elhmaidi, A. Provenzale, A. Babiano, Elementary topology of two-dimensional turbulence from a Lagrangian viewpoint and single-particle dispersion, J. Fluid Mech. 257 (1993) 533–558.
[15] A. Provenzale, Transport by coherent barotropic vortices, Annu. Rev. Fluid Mech. 31 (1999) 55–93.
[16] C. Basdevant, T. Philipovitch, On the validity of the "Weiss criterion" in two-dimensional turbulence, Physica D 73 (1994) 17–30.
[17] J. Jeong, F. Hussain, On the identification of a vortex, J. Fluid Mech. 285 (1995) 69–94.
[18] L. Zavala Sansón, G.J.F. van Heijst, Nonlinear Ekman effects in rotating barotropic flows, J. Fluid Mech. 412 (2000) 75–91.
[19] G.J.F. van Heijst, H.J.H. Clercx, S.R. Maassen, A note on the effects of solid boundaries on confined decaying 2D turbulence, in: O.U. Velasco Fuentes, J. Sheinbaum, J.L. Ochoa (Eds.), Non-linear Processes in Geophysical Fluid Dynamics, Kluwer, The Netherlands, 2003, pp. 305–324.
[20] J.P. Bourguignon, H. Brezis, Remarks on the Euler equation, J. Funct. Anal. 15 (1974) 341–363.
[21] E. Kreyszig, Differential Geometry, Dover, New York, 1991, p. 125.